Dissociable effects of reward and expectancy during evaluative feedback processing revealed by topographic ERP mapping analysis

Davide Gheza*, Katharina Paul*, & Gilles Pourtois

*Contributed equally to this work (shared first authorship)

Cognitive and Affective Psychophysiology Laboratory, Department of Experimental Clinical & Health Psychology, Ghent University, Ghent, Belgium

Corresponding author: Davide Gheza

Department of Experimental Clinical and Health Psychology, Ghent University

Henri Dunantlaan 2

9000 Ghent, Belgium

Phone: +32 9 264 86 15

E-mail: gheza.davide@ugent.be

Abstract

Evaluative feedback provided during performance monitoring (PM) elicits either a positive or negative deflection ~250-300 ms after its onset in the event-related potential (ERP) depending on whether the outcome is reward-related or not, as well as expected or not. However, it remains currently unclear whether these two deflections reflect a unitary process, or rather dissociable effects arising from non-overlapping brain networks. To address this question, we recorded 64-channel EEG in healthy adult participants performing a standard gambling task where valence and expectancy were manipulated in a factorial design. We analyzed the feedback-locked ERP data using a conventional ERP analysis, as well as an advanced topographic ERP mapping analysis supplemented with distributed source localization. Results reveal two main topographies showing opposing valence effects, and being differently modulated by expectancy. The first one was short-lived and sensitive to no-reward irrespective of expectancy. Source-estimation associated with this topographic map comprised mainly regions of the dorsal anterior cingulate cortex. The second one was primarily driven by reward, had a prolonged time-course and was monotonically influenced by expectancy. Moreover, this reward-related topographical map was best accounted for by intracranial generators estimated in the posterior cingulate cortex. These new findings suggest the existence of dissociable brain systems depending on feedback valence and expectancy. More generally, they inform about the added value of using topographic ERP mapping methods, besides conventional ERP measurements, to characterize qualitative changes occurring in the spatio-temporal dynamic of reward processing during PM.

Keywords: performance monitoring, reward processing, FRN, reward positivity, ACC, PCC

Introduction

Performance monitoring (PM) is crucial to foster goal adaptive behavior. According to most recent models (Ullsperger et al., 2014a) it is best conceived as a feedback loop whereby action values are learned and updated, especially when mismatches between goals and actions occur unexpectedly. Although these mismatches can sometimes be processed based on internal or motor cues (e.g., response errors), in many situations, external evaluative feedback provides the primary source of information to guide the course of PM. At the psychophysiological level, there has been a rich tradition of event-related brain potentials (ERP) research aimed at exploring the putative brain mechanisms underlying this loop during feedback-based PM.

Traditionally, the feedback-related negativity (FRN, sometimes termed FN, fERN, or MFN) was put forward as the main electrophysiological correlate of evaluative feedback processing during PM (Holroyd and Coles, 2002; Miltner et al., 1997; Ullsperger et al., 2014b; Walsh and Anderson, 2012). The FRN corresponds to a phasic negative fronto-central ERP component (N200) peaking around 250 ms after evaluative feedback (FB) onset, being typically larger for negative compared to positive outcome, as well as unexpected relative to expected one. This negative deflection is usually preceded by a positive ERP component (P200; Sallet et al., 2013), as well as followed by the P300, corresponding to a large positive deflection being maximal around 300-400 ms at central and posterior parietal scalp electrodes.

Initially, amplitude changes of the FRN (very much like the ERN, error-related negativity, which is time-locked to response onset) have been interpreted against a dominant reinforcement learning theory (RL-ERN theory; Holroyd and Coles, 2002; Sambrook and Goslin, 2015; Walsh and Anderson, 2012). In this framework, changes in the amplitude of the FRN capture indirectly dopaminergic-dependent reward prediction error signals (RPE; i.e. outcome either better or worse than expected). Moreover, the (dorsal) anterior cingulate cortex (dACC, sometimes termed rostral cingulate zone - RCZ; Ullsperger et al., 2014a) is thought to be the main intracranial generator of this phasic ERP component

(Gehring and Willoughby, 2002; Miltner et al., 1997; Yeung et al., 2004; Yu et al., 2011). According to the RL theory, the FRN reflects the processing of the outcome along a good-bad (valence/outcome) dimension, in relation to its actual expectancy. In other words, the FRN is thought to provide an integrated neural signal during PM where both the salience (absolute prediction error) and the valence (signed prediction error) of the outcome are integrated (Holroyd and Coles, 2002; Ullsperger et al., 2014). Consistent with this view, many ERP studies previously reported reliable changes of the FRN amplitude as a function of not only the valence of the feedback, but also its expectancy, usually manipulated by means of changes in reward probability across trials (for reviews, see San Martín, 2012; Walsh and Anderson, 2012).

More recently, researchers have begun to explore reward processing per se, as opposed to RPE. As a matter of fact, when the emphasis is put on reward processing at the feedback level (especially when monetary reward is used as main incentive), the amplitude difference seen at the FRN level (i.e. when reward is delivered vs. omitted) can be best explained by the generation of a positive activity associated with better than expected outcomes, rather than a negativity associated with worse than expected ones. In the existing ERP literature, this positivity has been named the "feedback correct-related positivity" (fCRP; Holroyd et al., 2008) or the "reward positivity" (RewP; Proudfit, 2015). It is elicited in the time range of the N200, and is thought to signal the achievement of the task goal (i.e. obtaining a reward) (Foti et al., 2011; Holroyd et al., 2008; Proudfit, 2015). In keeping with the RL-FRN theory, Holroyd et al. (2008) reinterpreted the N200 (Towey et al., 1980) giving rise to the FRN[1] as the neural signal indicating that the task goal has not been achieved. The N200 is usually elicited by task-relevant events in general (i.e. unexpected outcome regardless of its outcome, see also Ferdinand et al., 2012) and might thus be overshadowed by the concurrent positive deflection that is elicited by positive FB. Accordingly, given that the positive (RewP) and negative (FRN) deflections

[1] Here we refer to "FRN" as the negative deflection elicited by no-reward FB, and to "RewP" as the positive deflection (or lack of negative one) elicited by reward FB. For ease of reading, in Methods and Results sections we will refer solely to the scoring method adopted for quantifying both deflections.

overlap in time, it remains nowadays partly unclear which of them best captures systematic changes in reward processing at the feedback level as a function of reward expectancy (San Martín, 2012). Comparing ERP amplitudes at certain or pre-defined sites elicited by positive (reward) or negative (no-reward) FB implicitly assumes a similar source of the EEG signal accounting for them. As a matter of fact, the question remains whether the N200 component giving rise to the FRN is actually reduced for positive FB due to direct inhibition of the RCZ for example (Hajihosseini and Holroyd, 2013; Holroyd et al., 2011, 2008), or alternatively, from the superposition of another (non-overlapping) component, being reward-related primarily and best expressed by the RewP. In agreement with this latter interpretation, Foti et al. (2011) provided evidence that such a positive component could result from the activation of the putamen within the basal ganglia (but see the methodological objections raised by Cohen et al., 2011; and the following reformulation in Proudfit, 2015). Further, the same authors (Foti et al., 2015) recently argued that the FRN may be a blend of loss- and gain-related neural activities, possibly reflecting the contribution of partly distinct networks. At variance with this interpretation, other authors contend that the dACC provides the main (and most plausible) source of both ERP components, and is actually the only cortical brain region whose activation pattern is consistent with the observed modulation of their amplitude at the scalp level by valence and expectancy concurrently (Martin et al., 2009). Thus, a consensus about the neural generators of this FB-based ERP signal is currently lacking, and other potential sources have been put forward as well (among others, the ventral rostral anterior and posterior cingulate cortex; Luu et al., 2003; Nieuwenhuis et al., 2005).

Whereas the standard approach in ERP research consists of measuring the amplitude (and/or latency) of either the FRN or RewP at a few electrode positions, it usually falls short of confirming or disconfirming one of these competing assumptions, nonetheless. Using a standard ERP approach, it remains indeed impossible to confirm directly whether systematic changes in the amplitude of the FRN component occurs following local changes within the dACC with outcome valence and reward expectancy, or alternatively, another reward-related and non-overlapping component blurs this effect.

To address this question, the standard ERP analysis can be supplemented by an advanced topographic ERP mapping analysis informing about the actual expression of the scalp configuration in the time range of the FRN and RewP (Murray et al., 2008; Pourtois et al., 2008). Furthermore, possible neural generators giving rise to them can be estimated with appropriate source localization methods. However, caution is needed when interpreting EEG source estimations. Converging evidence obtained when crossing different imaging techniques (such as EEG and fMRI for example) could eventually help validate and confirm localization results based on EEG only, as performed here.

Following standard practice (Keil et al., 2014), an ERP component is usually defined not only by its polarity, amplitude and latency, but also by its actual topography and neural generators. Topography refers here to the actual spatial configuration of the electric field at the time where the ERP component of interest, here FRN and RewP, is best expressed at the scalp level, including all channels available concurrently. Noteworthy, changes in the topography necessarily denote changes in the underlying configuration of brain generators (Lehmann and Skrandies, 1980; Vaughan, 1982). Accordingly, characterizing ERP components accurately using complementing topographical evidence provides an important source of information regarding the actual (dis)similarity between conditions in terms of underlying brain networks; a level of analysis that cannot be reached directly when considering only the amplitude changes occurring at a limited number of electrode positions (usually Fz or FCz only in the case of the FRN). Further, some of these local amplitude changes can in principle be confounded or inflated by more global changes in the topography (and/or global strength) of the electric field across conditions, challenging the validity of some of the interpretations made when using a standard ERP analysis only. Moreover, local amplitude measurements at a few electrode positions strongly depend on the specific reference montage used. By comparison, the actual topography of an ERP component is reference-free (Murray et al., 2008). Additionally, a clear asset of recent topographical ERP mapping analyses (Michel and Murray, 2012) is that user/experimenter-related biases and priors can be strongly limited, including the selection of specific time-frames for further statistical analyses. In this framework, the main topographical components are revealed using a

stringent clustering method that allows to identify the specific time periods in the ERP signal where they are best expressed. As a result, there is no need to select a priori specific electrode locations or time-frames for statistical analyses, decreasing ultimately the likelihood of type I error (Luck and Gaspelin, 2017).

Surprisingly, to the best of our knowledge, the topography of the FRN and RewP components have not been scrutinized yet in the existing ERP literature. For example, it remains currently unclear whether the FRN and RewP share common topographical variance, or instead, can clearly be dissociated from one another when considering this global level of analysis, especially when a high density montage (64 channels or more) is used. Further, possible modulatory effects of reward expectancy on the topography of the FRN and RewP remain also poorly understood. However, such an analysis has the potential to address one of the main theoretical questions raised in the current ERP literature about these two ERP components and as reviewed here above: is the negative component (N200) giving rise to the FRN clearly different (at the topographical level) relative to the RewP? Moreover, considering the topography as level of analysis can also shed new light on the actual interplay of feedback outcome with feedback expectancy. These questions lie at the basis of the current study.

To address them and inform about reward processing during externally-driven PM, we recorded high-density (64 channels) EEG in 44 adult healthy participants while they performed a previously validated gambling task (Hajcak et al., 2005) where FB outcome (reward vs. no-reward) and expectancy (low, intermediate of high reward probability) were manipulated on a trial by trial basis using a factorial design. First, we carried out a standard ERP analysis and extracted the mean amplitude of the FRN and RewP, using and contrasting different scoring methods available in the literature: peak to peak vs. mean amplitude measurement. Second and crucially, we ran an advanced topographic ERP mapping analysis on the exact same average ERP data time-locked to FB onset, and isolated the dominant topographical components accounting for them, in an unbiased way. For the standard ERP

126 analysis, we surmised a larger FRN for no-reward compared to reward FB, with the opposite effect
127 found for the RewP, as well as a possible modulation of each of these two ERP components by
128 expectancy (i.e., larger amplitude for unexpected than expected outcome each time; Walsh and
129 Anderson, 2012). At the topographical level, we tested the prediction that the FRN and RewP could
130 lead to partly dissociable spatial configurations of the global electric field (i.e., topography), and hence
131 non-overlapping intracranial generators, as has been suggested before. More specifically, given that
132 the FRN is usually maximal at fronto-central scalp locations (for negative/no-reward FB) and was
133 previously related to the dACC (among others, Gehring and Willoughby, 2002; Miltner et al., 1997;
134 Yeung et al., 2004; Yu et al., 2011), we conjectured that topographical ERP variance associated with
135 no-reward could be associated with this specific brain region in our study. In comparison, since
136 positive/reward-related ERP activity during FB processing was previously linked to activation in more
137 posterior parts of the cingulate cortex (Cohen et al., 2011; Fouragnan et al., 2015; Nieuwenhuis et al.,
138 2005), and/or specific regions of the basal ganglia (Foti et al., 2015, 2011), we hypothesized that these
139 regions (especially the posterior cingulate cortex) could account for the reward-related activity during
140 feedback processing in our study. Furthermore, we sought to explore whether these two spatial
141 configurations of the electric field depending on FB outcome, if clearly dissociable from one another,
142 could show a similar or instead different sensitivity to FB expectancy.

Methods

Participants

Existing EEG data from two previous (and separate) studies by Paul and Pourtois (2017 - Experiment 1) and Gheza et al. (submitted – Experiment 2), where the same gambling task was used, were pooled together. A total of forty-five undergraduate students from Ghent University (right-handed, with normal or corrected-to-normal vision, and no history of neurological or psychiatric disorders) were included in the present study. They all gave written informed consent prior to the start of the experiment and were compensated about 30€ for their participation. The study by Paul and Pourtois (2017) had a between-groups design and involved a mood-induction paradigm. Only the control group (with a neutral-mood state, 25 participants) from this study and the whole sample (20 participants) from Gheza et al. (submitted, where no specific mood induction was used) were merged together. One participant had to be excluded due to noisy EEG recording. Hence, the total sample included 44 participants (34 females, age: *M* = 22.0 years, *SD* = 2.6). Both studies were approved by the local ethics committee at Ghent University. A post hoc power analysis was conducted using GPower (Faul et al., 2007). The sample size of 44 was used for the statistical power analyses and the power to detect a small (η^2=0.01), medium (η^2=0.06) or large (η^2=0.14) effect for the interaction between valence and expectancy was estimated. The alpha level used for this analysis was set to .05. The post hoc analyses revealed the statistical power for this study was .22 for detecting a small effect, .91 for detecting a medium effect size, and exceeded .99 for a large effect. Thus, this sample size was more than adequate to detect a moderate/large effect, but not a small one.

Stimuli and task

A previously validated gambling task (Hajcak et al., 2007) was adapted and administered in both studies. On each and every trial, participants had to choose one out of four doors by pressing with their right index finger the corresponding key on the response box. After a fixation dot (700 ms) this choice was followed by either positive FB (green “+”), indicating a win, or no-reward FB (red “o”)

(1000 ms). The two studies differed slightly in the amount of monetary reward, being either 8 cents (Paul and Pourtois, 2017) or 5 cents (Gheza et al., submitted). At the beginning of each trial, participants were informed about reward probability with a visual cue (600 ms), followed by a fixation dot (1500 ms). This cue was presented in the form of a small pie chart shown at fixation. Either one, two or three quarters were filled (black/white) corresponding to a reward probability of 25, 50 or 75 %. A reward probability of 25% indicated that only one door contained the reward, two doors in the case of 50% reward probability and three doors for 75% reward probability. Unbeknown to participants, the outcome was actually only related to these objective probabilities (but not the actual choices made by them), ending up with a preset winning of €14.72 (Paul and Pourtois, 2017) or €12.40 (Gheza et al., submitted). Inter trial interval was fixed and set to 1000 ms. Hence, by crossing the three possible reward probabilities with the two opposite outcomes, six trial types were included in a factorial design[2]. To ensure participants paid attention to the cue and outcome, catch trials were randomly interspersed in the trial series. In 24 trials, at the cue offset they were asked to report their winning chance ("how many doors contain a prize?", allowing responses from 1 to 3). In 24 different trials, they were asked about the expectedness of the outcome at FB offset, and answers were collected by means of a visual analog scale (VAS) anchored with "very unexpected" and "very expected".

All stimuli were shown against a grey homogenous background on a 21-in CRT screen and controlled using E-Prime (V 2.0, Psychology Software Tools Inc., Sharpsburg, PA).

Procedure

In both studies, after reading the instructions, participants were first familiarized with the gambling task using 12 practice trials. The presentation of the 6 trial types (3 reward probabilities x 2 outcomes) was randomized, and the same trial type could be presented consecutively. The main

[2] Beside the conditions described above ("regular" trials), the task for Gheza et al. (in preparation) also included "special" trials, that were discarded from the analyses conducted in the present study.

experiment consisted of four blocks each comprising 92 (Exp. 1 – Paul and Pourtois, 2017) or 124 trials (Exp. 2 – Gheza et al., submitted). After each block, a short break was included and participants were informed about their current (cumulative) payoff.

In Paul and Pourtois (2017), a total of 368 trials was presented (80 with 50%, 144 with 25% and 144 with 75% reward probability). A neutral-mood induction procedure was applied before the task and repeated after each block to maintain the specific mood state (here neutral) throughout. In Gheza et al. (submitted), a total of 392 trials was used (104 with 50%, 144 with 25% and 144 with 75% reward probability).

Recording and Preprocessing of Electrophysiological Data

EEG was recorded using a 64-channel Biosemi Active Two system (http://www.biosemi.com) with four additional electrodes measuring horizontal and vertical eye movements. EEG was sampled at 512 Hz and referenced to the Common Mode Sense (CMS) active electrode and Driven Right Leg (DRL) passive electrode. The EEG was preprocessed offline with EEGLAB 13.5.4b (Delorme and Makeig, 2004), implemented in Matlab R2012b. A 0.05/35 Hz high/low pass filter was applied after re-referencing the EEG signal to the averaged mastoids. An independent component analysis was run on the continuous data to correct manually for eye artifacts and spatial or temporal discontinuities. Individual epochs were extracted from -250 to 750 ms around the FB onset and a pre-feedback baseline was subtracted (-250 to 0). A semi-automatic artefact correction procedure was applied to eliminate trials with voltage values exceeding ± 90 µV or slow voltage drifts with a stronger slope than ± 90 µV, as well as based on visual inspection. For each subject separately, artefact-free epochs were grouped according to the six main experimental conditions: expected, no-expectations[3] and unexpected FB associated with reward (deriving from 75%, 50%, 25% reward probability trials respectively), or expected, no-expectations and unexpected FB associated with no-reward (deriving from 25%, 50%,

[3] The no-expectation term refers here to the objective reward probability and not the subjective expectation or uncertainty. The condition provides equal (objective) probability of reward or no-reward FB and therefore goes along with the highest uncertainty regarding feedback outcome during the experiment.

75% reward probability trials respectively). To avoid different signal to noise ratios between conditions, the same number of trials (randomly sampled) was used for all of them, being defined subject-wise based on the condition with the lowest trial count.

Standard peak analysis

FRN: peak to peak. The FRN and RewP were determined peak-to-peak at FCz (FRN-pp) as the difference between the most negative peak (N200: within 200 - 350 ms) and the preceding positive peak (P200: within 150 - 250 ms) assumed as the onset of the (relative) negativity (Holroyd et al., 2008, 2003).

FRN: mean amplitude. We also used an alternative scoring method for the FRN and RewP (FRN-m), defined at FCz as the mean amplitude within the 213-263 ms interval post-feedback onset (i.e. the 50 ms window surrounding the peak of the N200 for no-reward; Novak and Foti, 2015; see also Weinberg and Shankman, 2017 for the use of a mean-amplitude approach in a different time window). This time window and location were based on the FRN-pp maximal amplitude from the grand average of no-reward FB trials (merging all three expectancy levels; "collapsed localizer" approach, see Luck & Gaspelin, 2016).

P2 and N2. Supplementary peak analyses on P200 and N200 components (when considered separately) were carried out in order to verify their relative sensitivity to FB expectancy and its interaction with FB valence. In accordance with the FRN-pp scoring method, P200 was defined as the maximum positivity occurring within the 150-250 ms interval post FB onset, while the N200 as the maximum negativity within the 200-350 ms interval post FB onset.

Topographical ERP mapping analysis (TA)

The dominant topographies accounting for the ERP data set under scrutiny were extracted using CARTOOL software (Version 3.60; developed by D. Brunet, Functional Brain Mapping Laboratory, Geneva, Switzerland). The basic principles of this method have been described extensively elsewhere (Brunet et al., 2011; Michel et al., 1999; Murray et al., 2008; Pourtois et al., 2008). In short, it is based

on two successive data analysis steps. First, the dominant topographical maps are isolated from the grand average ERP data by means of a clustering algorithm that takes into account the global dissimilarity, i.e. the difference in terms of spatial configuration between two normalized maps independent of the global strength of the ERP signal (Lehmann and Skrandies, 1980). Next, these main and dissociable topographical configurations are fitted back to the individual subject ERP data and a quantification of their representation across subjects and conditions is then provided, including the global explained variance (or goodness of fit), the correlation and the time point of the best fit. Parametric tests are eventually performed on these variables in order to compare different experimental conditions at the statistical level.

TA: Segmentation. First, using a competitive T-AAHC cluster analysis (Topographic - Atomize and Agglomerate Hierarchical Clustering) (Brunet et al., 2011; Tibshirani and Walther, 2005) of the entire epoch (i.e. from -250 prior to and up to 750 ms following feedback onset, corresponding to 512 time frames-TFs at a 512-Hz sampling rate), the dominant topographical maps were identified. The specific (and default) settings for the clustering method followed the recommendations implemented in CARTOOL and were the following. 1) Minimum and maximum number of clusters were predefined to one and nine, 2) a smoothing kernel (Besag factor 10), of three TFs was applied, and 3) segments shorter than three TFs were rejected. The choice of the best segmentation result was based on an objective meta criterion of 7 criteria proposed previously (see Charrad et al., 2014) and visual inspection of the results.

TA: Fitting. The dominant topographies identified in the preceding step were then fitted back to the individual averages (n=6 per subject) to determine their expressions across participants and conditions. As the focus of the analysis was on reward processing (and expectancy), we mostly examined possible changes in the topography of the ERP signal as a function of reward and/or expectancy occurring 200-500 ms post-feedback onset, in keeping with many previous ERP studies (Foti et al., 2015; Hajcak et al., 2007; Sambrook and Goslin, 2015; Ullsperger et al., 2014b). Fitting

parameters also followed the recommendations implemented in CARTOOL and included 1) a smoothing kernel (Besag factor 10) of three TFs and 2) rejection of segments shorter than three consecutive TFs. The fitting procedure was done as a non-competitive process to validate that one of the topographic configurations fitted better than the other one depending on the condition (based on global explained variance - GEV - and the mean correlation of the map with the signal). Furthermore, the time course of these topographic maps could be evaluated, i.e. the TF of the best correlation could be compared between the maps and across conditions. If the last approach revealed a significant temporal difference between the dominant maps, the fitting procedure was repeated separately for the different time windows.

Source Localization

To estimate the configuration of the neural generators underlying the previously identified reward related topographical maps, a distributed linear inverse solution was used—namely, standardized low-resolution brain electromagnetic tomography (sLORETA; Pascual-Marqui, 2002). sLORETA solutions are computed within a three-shell spherical head model coregistered to the MNI152 template (Mazziotta et al., 2001). LORETA estimates the 3-D intracerebral current density distribution within a 5-mm resolution. The 3-D solution space is restricted to the cortical gray matter and hippocampus. The head model uses the electric potential field computed with a boundary element method applied to the MNI152 template (Fuchs et al., 2002). Scalp electrode coordinates on the MNI brain are derived from the international 5% system (Jurcak et al., 2007). The calculation was based on the conditions specific average per subject in the time window of interest identified in the previous analysis.

Statistical Analysis

At the behavioral level, the subjective ratings related to catch trials after the FB (probing FB expectation) were first transformed to percentages, arbitrarily setting one anchor (‘very unexpected’) to 0 and the other one (‘very expected’) to 100. These evaluations were considered to be correct if

they fell within a ± 25% range around the correct response (see Paul and Pourtois, 2017 for a similar procedure). The amount of correct responses to these catch trials as well as catch trials corresponding to the cue (probing reward probability) were eventually reported as percentage of correct responses.

At the ERP level, repeated measures ANOVAs with FB expectancy (expected, no-expectations, unexpected) and outcome (reward vs. no-reward) as within-subject factors were performed (individual trial count, balanced across the six conditions: *M* = 27.4, *SD* = 4.3) separately for FRN-pp and FRN-m.

At the topographical level, each of the three dependent variables gained by the fitting procedure (i.e., GEV, mean correlation, TF of best correlation) was entered in a 2 x 3 x 2 repeated measurement ANOVA with the within-subject factors map configuration (FRN vs. RewP-map), expectancy (unexpected, no-expectations, expected) and FB valence (reward vs. no-reward). If the previous analysis based on TF of best correlation hinted at a potentially interesting difference in the time-course of the main maps, another ANOVA was run with the same within-subject factors, but adding a factor "time-window"(early vs. late).

The inverse-solution results were compared between the two reward outcomes (reward vs. no-reward) using paired-sample t-tests performed on the log-transformed data. To reveal potential differences in the inverse-solution space through direct statistical comparison, a stringent nonparametric randomization test was used (relying on 5,000 iterations, see Nichols and Holmes, 2001).

For all analyses, significance alpha cutoff was 0.05.

Results

Behavioral Results

The accuracy for the cue ($M_{correct}$= 88.1 %, *SD* = 8.0) and for the outcome evaluation ($M_{correct}$ = 60.7 %, *SD* = 25.3), as inferred from the catch trials, were high and well above chance level, suggesting

313 that participants correctly monitored reward probability (based on the visual cue) and outcome (based
314 on the feedback).

315 **ERP Results**

316 **FRN: peak to peak.** The analysis performed on the FRN-pp amplitudes showed a significant
317 main effect of FB valence ($F(1, 43) = 16.78$, $p < .001$, $\eta^2 = .281$) and an interaction between FB valence
318 and FB expectancy ($F(2, 86) = 12.49$, $p < .001$, $\eta^2 = .225$). The FRN component was larger (more
319 negative) for no-reward compared to reward FB ($M_{reward} = -5.08$, $SE = 0.30$, $M_{no\text{-}reward} = -6.55$, $SE = 0.36$).
320 The multivariate simple effect of FB expectancy was significant for no-reward ($F(2, 42) = 7.06$, $p = .002$,
321 $\eta^2 = .252$), but not for reward FB ($F(2, 42) = 1.65$, $p = .203$, $\eta^2 = .073$), confirming its sensitivity to RPE,
322 when scored peak to peak[4] (see Fig. 1).

323 **FRN: mean amplitude.** The analysis performed on the FRN-m amplitudes showed a significant
324 main effect of FB valence only ($F(1, 43) = 62.39$, $p < .001$, $\eta^2 = .592$), without a significant interaction
325 between FB valence and FB expectancy, however ($F(2, 86) = 2.19$, $p = .118$, $\eta^2 = .048$). The FRN-m was
326 larger (more negative) for no-reward compared to reward FB ($M_{reward} = 2.42$, $SE = 0.51$, $M_{no\text{-}reward} = -$
327 0.41, $SE = 0.44$). These results indicated that, on this critical time window and fronto-central channel,
328 the FRN, when scored using a stringent mean amplitude measurement, was sensitive to FB valence
329 only (reward being present or absent), without any significant modulation due to FB expectancy (see

[4] In order to rule out that these neurophysiological effects were different between the two samples, we used a Bayesian factor analysis which is suited for estimating the amount of evidence in favor or against the null hypothesis (Rouder et al., 2017). More specifically, the data from the FRN-pp method was examined in a Bayesian repeated measure ANOVA in which the factors were FB outcome (reward or no-reward), FB expectancy (expected, no-expectations, or unexpected) and Group (Exp 1 or Exp 2). We used the JASP software package (JASP Team, 2017 - version 0.8.1.2) with default prior settings. First, the likelihood for each alternative models (derived from the combination of the 3 factors) was tested against a Null model. The models that best explained the variance were the main effect of Outcome, followed by the one including the two main effect of Expectancy and Outcome and their interaction (BF10 for Outcome = 40266, BF10 for Expectancy + Outcome + Expectancy * Outcome = 9031). In order to rule out the Group factor effects, we then included the model terms Expectancy, Outcome and Expectancy * Outcome (i.e. flagged as Nuisance) in every model (including the Null model) and we looked at the BF01 (likelihood of the Null model over the others). The Null model (assumed probability of 1) was 6.8 times more likely to be true compared to the model including the main effect of Group (BF10 = 0.145), and much more likely compared to any other model that included an interaction with Group (BF10 < 0.068). These results provide moderate to very strong evidence for the absence of a Group effect on these FRN-pp results.

Figure 1). Hence, these results suggest a qualitatively different outcome at the FRN level depending on the specific scoring method used.

P2 and N2. Repeated measure ANOVAs were run on the two components separately, with FB valence and FB expectancy used as within subject factors. The analysis for the P200 revealed significant main effects of Valence ($F(1, 43) = 9.23$, $p = .004$, $\eta^2 = .177$) and Expectancy ($F(2, 86) = 4.49$, $p = .014$, $\eta^2 = .095$). The analysis on the N200 revealed a significant main effect of Valence ($F(1, 43) = 47.64$, $p < .001$, $\eta^2 = .526$) and crucially, a significant interaction between Valence and Expectancy ($F(2, 86) = 6.45$, $p = .002$, $\eta^2 = .130$). Thus, although the FRN-pp scoring method could potentially inflate the effect of Expectancy driven by the P200 (as opposed to N200) component, it is clear from the N200 only analysis that this deflection alone was significantly modulated by both factors concurrently in our study.

Topographic Analysis

Segmentation. Following the meta-criterion, a solution with sixteen different dominant maps was found to explain the ERP data set the best. The solution explained 93.71 % of the variance, see Figure 2. During the time window corresponding to the FRN and RewP, two different dominant maps were clearly evidenced. One map, sharing similarities with the FRN ERP component, showed a fronto-central negativity and started at a similar time point (i.e. 217 ms) regardless of feedback expectancy's level, but only for negative FB. Moreover this distinctive map was immediately followed by a different map showing a broader central positivity. This RewP-map was present and lasted until the same time point for all six FB types (i.e. 386 ms). The spatial correlation between these two maps was 0.84.

Fitting. The extracted the GEV and the mean correlation, provided by the fitting of the two dominant maps in the time window of interest (217 – 386 ms) revealed a significant main effect of map ($F(1, 43) \geq 9.04$, $p \leq .005$, $\eta^2 = .17$). Both variables showed a significant interaction between FB valence and map ($F(1, 43) \geq 34.47$, $p < .001$, $\eta^2 \geq .45$) and FB expectancy and map ($F(2, 86) \geq 7.86$, $p \leq .001$, $\eta^2 \geq .16$), see Figure 3. While the RewP-map explained more variance and showed a higher mean correlation for reward than no-reward FB ($M_{\text{reward-meanCorr}} = .70$, $SE = .02$, $M_{\text{no-reward-meanCorr}} = .63$, $SE = .02$,

$p \leq .002$), the FRN map showed only a non-significant trend to fit better with the no-reward compared to the reward FB ($M_{\text{reward-meanCorr}} = .57$, SE = .03, $M_{\text{no-reward-meanCorr}} = .60$, $SE = .03$, $p \geq 0.25$). Regarding the GEV, both maps seemed to be sensitive to the expectancy manipulation as well. More variance was explained for the unexpected than the expected condition (FRN-map: $M_{\text{unexpected}} = .08$, $SE = .006$, $M_{\text{expected}} = .06$, $SE = .005$, $p \leq 0.05$). Especially the positivity map showed a steeper increase with unexpectedness (positivity map: $M_{\text{unexpected}} = .10$, SE = .006, $M_{\text{expected}} = .07$, $SE = .004$, $p < .001$). For the mean correlation, the RewP-map showed a similar pattern ($M_{\text{unexpected}} = .68$, $SE = .02$, $M_{\text{expected}} = .65$, $SE = .02$, $p < .015$), while the FRN-map did not differentiate between levels of expectancy ($M_{\text{unexpected}} = .58$, $SE = .03$, $M_{\text{expected}} = .58$, $SE = .03$, $p \geq 0.34$).

Importantly the TF of the best correlation for each map within this time large segment showed again a significant interaction between map and FB valence ($F(1, 43) = 8.31$, $p = .006$, $\eta^2 = .16$), indicating that for reward FB, both maps fitted equally well at 306 ms ($M_{\text{FRN-map}} = 305$ ms, $SE = 7.69$, $M_{\text{RewP-map}} = 307$ ms, $SE = 6.04$, $p = .81$), while for no-reward FB, the FRN-map fitted the best much earlier than the RewP-map ($M_{\text{FRN-map}} = 277$ ms, $SE = 6.97$, $M_{\text{RewP-map}} = 318$ ms, $SE = 5.79$, $p < .001$). This result clearly indicated that the initial time window of interest (217 – 386 ms) was probably too broad and likely encompassed two dissociable processes in terms of spatial-temporal dynamic. To corroborate this assumption at the statistical level, we repeated the fitting within two short non-overlapping time windows lasting for 40 ms centered around 277 and 318 ms, respectively. The repeated measures ANOVA on the GEV values revealed, besides several significant main effects, two significant three way interactions between time-window, map and FB valence ($F(1, 43) = 66.37$, $p < .001$, $\eta^2 = .61$) and time-window, map and FB expectancy ($F(2, 86) = 5.01$, $p = .009$, $\eta^2 = .10$), see Figure 4. Whereas the FRN-map fitted the best in the early time window for no-reward FB ($M_{\text{no-reward-early}} = .07$, SE = .007, $M_{\text{no-reward-late}} = .06$, $SE = .006$, $p \geq .139$), the RewP-map fitted the best for reward FB in the later time window ($M_{\text{reward-early}} = .07$, $SE = .006$, $M_{\text{reward-late}} = .10$, SE = .006, $p \leq .059$). Furthermore, while the FRN-map did not vary with expectancy for none of the two time windows ($M_{\text{unexpected}} = .07$, $SE = .006$, $M_{\text{expected}} = .06$, $SE = .006$, $p \geq .139$), the positivity map showed this effect, especially in the later time window

($M_{unexpected\text{-}late}$= .11, *SE* = .006, $M_{expected\text{-}late}$= .08, *SE* = .005, $p \leq .003$). Using the mean correlation as fitting parameter, as opposed to the GEV, led to a similar statistical outcome.

Source Localization

The statistical comparison in the inverse-solution space between reward an no-reward within the time window of the FRN- and RewP-map (217-386 ms) revealed two non-overlapping suprathreshold (*t* value > 4.13, corrected for multiple comparisons) clusters showing opposing reward-related effects, see Figure 5. One cluster, being more active for no-reward than reward FB, was located within the dACC, including Brodmann area (BA) 32; (maximum at 15x, 25y, 40z, $t(43) = -5.31$, $p < .001$) and spreading to adjacent frontal areas, including BAs 6, 8 and 9. The other non-overlapping cluster showed the opposite pattern (more active for reward than no-reward FB) and was located in the posterior cingulate cortex (PCC; BA 23; maximum at -5x, -60y, 15z, $t(43) = 5.85$, $p < .001$), extending to adjacent (medial) parietal regions (such as the Precuneus or retrosplenial cortex; BA 31), as well as more ventrally to the posterior part of the Parahippocampal gyrus (BA 27). It also spread to the posterior part of the left insula (BA 13; max. at -30x, -40y, 20z, $t(43) = 4.89$, $p < .001$).

Discussion

RPE signals recorded at the electrophysiological level during PM are thought to provide an integration of expectancy and valence of the outcome, such that a differential response to rewarding vs non-rewarding outcome increases as a function of its unpredictability (Holroyd and Coles, 2002; Schultz et al., 1997). If the evidence for a mismatch between expectation and outcome is motor based (e.g., clear response error), then such an effect can be tracked at the level of response-locked ERPs, such as the ERN. However, if the evidence cannot be computed at the response level (e.g., during gambling or probabilistic learning), then FB provides the main source of information to estimate RPE, with neurophysiological effects visible at the level of the FRN/RewP. The present study focussed on this

latter effect. More specifically, we aimed to characterize the topographical properties of the FRN component, when compared to the RewP, in order to assess whether they share common or instead dissociable topographic variance and neural generators. Importantly, we could compare the outcome of this data-driven method (taking into account all electrodes and time-frames) to two standard ERP scoring methods available in the literature, focussing on a circumscribed time-window and FCz electrode only.

To this aim, 44 participants carried out a previously used gambling task (Hajcak et al., 2007; Paul and Pourtois, 2017), where FB valence and expectancy were manipulated on a trial-by-trial basis, while 64-channels EEG was recorded concurrently. This enabled us to estimate the contribution of these two independent variables to systematic changes in the ERP signal following FB onset, when it corresponded either to amplitude modulations recorded at FCz only, or alternatively, when considering the spatial configuration of the entire electric field (i.e., topography). A number of new results emerge from the current study. (i) When comparing two different, albeit standard, scoring methods for the FRN in the existing ERP literature, our results show that this component was reliably modulated by FB valence and expectancy when using a peak to peak measurement only (FRN-pp, i.e., measuring peak amplitude of the N200 relative to the preceding P200 at FCz component). Importantly, a similar outcome was reported when measuring the N200 alone. By comparison, when we used a more stringent mean amplitude measurement at the same lead (FCz) (FRN-m, i.e., measuring FRN as a mean ERP activity spanning from 213 to 263 ms interval centered around the N200 peak), it was modulated by valence without significant change by expectancy, suggesting in turn a dissociation between them. (ii) These somewhat inconsistent results were supplemented with a topographical pattern analysis that strongly reduced the number of priors in terms of location and latency for identifying reward-related effects following FB onset, and possible interactions with expectancy. This analysis unambiguously showed the existence of two dissociable topographies during the time-interval corresponding to the FRN and RewP. A main topography characterized by a short-lasting prefrontal negative component was generated relatively early after negative FB onset and was somehow

independent from its expectancy. Another one showed a broad positivity at more central and parietal sites during the same early time interval, and was generated in response to reward. Crucially, this latter reward-related topography lasted longer and best represented the variance of the ERP signal in a later time window, where it also varied systematically as a function of reward expectancy, accounting for more variance for unexpected than expected positive FB, in agreement with the tenets of the dominant RPE framework (Schultz, 2013). Given these specific electrophysiological properties and opposing sensitivity to FB valence, we tentatively linked the first one to the FRN and the second one to the RewP, when corresponding to local amplitude variations of specific deflections measured at a single scalp channel. Because different topographies necessarily denote non-overlapping intracranial generators (Lehmann and Skrandies, 1980; Michel and Murray, 2012; Vaughan, 1982), we estimated their sources using a linear inverse solution algorithm (sLoreta, see Pascual-Marqui, 2002). While the FRN-compatible topographical activity had a main cluster within the dACC, the RewP-one was source localized to a distributed and extended network, comprising primarily the PCC. Here below, we discuss the implications of these new results, and eventually formulate some recommendations for the definition and use of feedback-based reward-related ERP activities in future studies.

At FCz scalp location, independently of the scoring method adopted and actual definition used for the ERP component of interest (either local amplitude changes or topography), we consistently found across these different methods used that the FRN amplitude varied reliably with valence, i.e. it was consistently larger for no-reward than reward FB, while conversely, the RewP amplitude was systematically larger for reward than no-reward FB. Noteworthy, the FRN component was sensitive to FB expectancy only when using a peak to peak analysis (FRN-pp). Thus the peak to peak scoring method was the only one with which the FRN was found to be coherent with the generation of a dopamine-dependent RPE signal (Holroyd et al., 2003; Holroyd and Coles, 2002; Schultz et al., 1997; Ullsperger et al., 2014b). No such modulation was found for the RewP, no matter which ERP scoring method was actually adopted. In light of the existing debate in the ERP literature about the sensitivity of the FRN, or instead RewP to FB expectancy (bearing in mind that these two hypotheses are not necessarily

458 mutually exclusive and are both consistent with the original FRN-RL theory; see Holroyd et al., 2008;
459 San Martín, 2012), our results lend support to the classical FRN hypothesis (Holroyd and Coles, 2002;
460 Ullsperger et al., 2014b; Walsh and Anderson, 2012).

461 When the FRN was scored as mean amplitude around the peak of the N200 (FRN-m), no reliable
462 modulation by FB expectancy was found. This inconsistency across the two scoring methods might be
463 explained by several factors. On one hand, the peak to peak measurement may have artificially inflated
464 the component's amplitude due to noise in the data (Luck and Gaspelin, 2017). On the other, scoring
465 the FRN using the mean amplitude computed for a relatively long and pre-defined time window, albeit
466 being a more conservative approach that is less sensitive to noise in the measurement, might have
467 overshadowed an effect of expectancy due to inter-individual variability in the latency (and
468 morphology) of the P200-N200-P300 complex, and/or to the possible temporal overlap of the N200
469 with the preceding P200 and/or the following P300. The N200 is usually flanked by these two positive
470 components, which usually do show amplitude modulations with stimulus frequency, and thus
471 expectancy (Donchin and Coles, 1988; Polich et al., 1996), although with an affect going in the opposite
472 direction compared to the N200. Neglecting these features of the ERP signal can in turn potentially
473 smear amplitude effects which are small in size, such as the expectancy effect on the FRN. Indeed, the
474 peak to peak approach (FRN-pp, where preceding P200 is used as baseline peak for N200 peak
475 measurement) was put forward as an alternative scoring method to control for this confounding effect
476 (Holroyd et al., 2003; Sallet et al., 2013). Notably, by further exploring amplitude modulations brought
477 about by FB expectancy (and valence) for each deflection separately (i.e., P200 and N200), we could
478 confirm that the significant interaction effect between FB valence and FB expectancy at the N200 level
479 (hence FRN) was not merely resulting from the preceding P200 (see Results). As a rule of thumb,
480 depending on the experimenter's goal and research interest, one of the two scoring methods could be
481 preferred above the other one. For instance, if the focus is on reward itself, the use of the FRN-m
482 appears warranted. By comparison, if more subtle influences of expectancy are explored at the FB (and
483 FRN) level, then a FRN-pp scoring method appears more appropriate than the FRN-m. However, in light

of these slight discrepancies between the different scoring methods used, and for comparison purposes with previous work in the literature, it appears important to report and compare the outcome of these different scoring methods when it comes to assessing the sensitivity of an ERP component, like the FRN or RewP, to FB valence and expectancy.

Although these classical peak analyses informed about the complex interplay between reward and expectancy during feedback-based PM, yet they are necessarily based on local amplitude variations only (here measured at FCz), and as such, they could therefore potentially overlook more global changes in the ERP signal occurring with these two factors, including topographical alterations. To explore this possibility, we supplemented these analyses with a topographical ERP mapping analysis that considered the FB-locked ERP signal when measured at all (64) electrodes concurrently, and during a large time interval following FB onset (hence, not restricted to local peaks or maxima only), reducing in turn strongly the number of priors. This analysis confirmed the presence of a clear topographical change depending on actual FB outcome during the time interval usually associated with the FRN or RewP. Whereas a main topography shared many similarities with the FRN component (no-reward dominance), the other competing spatial configuration of the electric field closely resembled what is usually referred to as RewP in the existing ERP literature and showed enhanced activity for reward. Moreover, source estimation using sLoreta confirmed the presence of two non-overlapping networks accounting for these two dissociable maps. As predicted by many models and earlier ERP studies (Bush et al., 2000; Fouragnan et al., 2015; Gehring and Willoughby, 2002; Miltner et al., 1997; Shackman et al., 2011; Ullsperger et al., 2014b), we found that the dACC provided the main intracranial generator of this FRN-compatible map. In comparison, the RewP activity was source localized to more posterior regions, including the PPC, an area known to be involved in reward processing (Knutson et al., 2001; Liu et al., 2011; Luu et al., 2003; Nieuwenhuis et al., 2005). Even though some caution is needed in the interpretation of these source localization results (as they correspond to imperfect mathematical reconstructions of the intracranial sources), this dissociation along the cingulum depending on FB valence is not odd, but very much in line with the taxonomy of functionally-distinct

sub-regions composing it, as previously put forward by Vogt (2005). In this framework, the anterior midcingulate cortex (aMCC) is linked with the processing of negative emotions (and the need for cognitive control, see Shackman et al., 2011), especially fear, anxiety, and even pain. Conversely, the PCC is assumed to play a predominant role in attention control, especially in orienting to targets that are potentially of high motivational value for the individual, in integrating the history of rewards previously experienced, as well as in the assessment of personal relevance of incoming (emotional) information, and controlling the balance between internal and external attention (Leech and Sharp, 2014). Using this neuro-anatomical framework, we could thus conjecture that the stronger aMCC response to no-reward FB in our study might reflect an (whole or none) alarm or alert signal in case the outcome turns out to be relatively "negative" (no-reward) (Shackman et al., 2011). In comparison, the stronger PCC activation to reward FB seems consistent with an attentional orienting effect towards an approach-related or motivationally significant event for the participant, namely getting a small financial reward after gambling in the present case. Similar interpretations of related findings have been drawn in the context of error monitoring (Paul et al., 2017) and reinforcement learning (Fouragnan et al., 2015).

Turning to the possible changes of these global ERP activities with FB expectancy, our topographical analysis additionally showed a striking modulation that none of the two classical ERP analyses (using FCz only) could actually reveal. Not only was FB valence clearly modulating the expression of the global electric field, but FB expectancy influenced its expression as well and in a condition-specific manner. As our analysis revealed (see Figure 2), the RewP-related map appeared to be the default ERP activity somehow in this long interval (from 210 to 380 ms following FB onset), progressively building up across this specific interval and reaching its maximum at ~320 ms following FB onset. No-reward outcome turned out to "break up" this default processing at an early latency (~280 ms following FB onset), with the generation of a unique and distinctive topography (being also short-lived), namely the FRN map. This result supports the idea that in case of a "negative" event (here corresponding to the lack of reward), a phasic negative ERP activity similar to the N200-component

(Heydari and Holroyd, 2016; Shahnazian and Holroyd, 2017) is elicited, which temporarily overrides the standard (reward-driven) ERP response. Although remaining largely speculative, this break-up effect might be caused by a phasic dip or transient pausing in dopaminergic firing, as the RL-theory would suggest (Fiorillo et al., 2003; Schultz, 2013; Warren and Holroyd, 2012). At variance with this interpretation, a positivity associated with better than expected positive outcome (Proudfit, 2015) could have been overridden by a more generic brain response to salient events in general (Holroyd et al., 2008; Talmi et al., 2013). Importantly, in line with the FRN-m analysis, this FRN-compatible topographical map did not show however a systematic modulation (in explained variance) with expectancy. We may speculate that both the FRN-m and the topographic mapping for the FRN map overlook a phasic, short-lived, local modulation of expectancy that only the FRN-pp and the N200 peak analyses were able to capture. Such a modulation was well evidenced in our topographic ERP mapping analysis, but for the RewP-related topography and at a later time point, however. Accordingly, these topographical results inform about the actual spatio-temporal dynamic of reward processing, suggesting that early on following FB onset, FB valence mostly influenced the expression of the ERP signal (irrespective of expectancy). In the present case, this FB valence effect was characterized by the transient blocking of the (normal) reward-related activity and replacement for a short period of time by another, negative or loss-related, ERP activity sharing many similarities with the FRN. Because our ERP results suggest the existence of two separate and dissociable networks depending on actual FB valence (yet having both an early time-course following FB onset), they clearly speak against the use of difference waves, where a new and undefined ERP activity would likely be created as a result of this transformation, in case no-reward would be subtracted from reward FB for example. Such an approach, although possibly reducing the number of factors/variables included in the statistical analysis (Luck and Gaspelin, 2017), would nonetheless overlook and mitigate the existence of independent sources and effects that each contributes to both (local) amplitude as well as (global) topographical changes in the ERP signal following FB onset. Hence, a clear methodological implication

of our new ERP results is that the use of difference waves should not be recommended as it could blur or smear important differences between the processing of reward vs. no-reward outcome during PM.

As mentioned here above, we succeeded to evidence systematic modulations of the feedback-locked ERP signal with expectancy with the elected topographic ERP mapping analysis. They were found for the RewP-related map exclusively, and became stable at the statistical level when considering a later time interval following FB onset (compared to the FRN map). Interestingly, the PCC and adjacent areas which are thought to give rise to this ERP activity, has previously been shown to be involved in detecting novel, or unpredicted events (Gabriel et al., 2002; Mccoy et al., 2003). Moreover, earlier ERP studies already clearly showed that during a comparable time window following FB onset, the amplitude of the RewP was modulated by expectancy and hence RPE (Sambrook and Goslin, 2015; Talmi et al., 2012). Accordingly, given this clear modulation of the ERP signal with expectancy for the RewP-related map, our novel results lend indirect support to earlier studies and models available in the ERP literature that posited that effects of expectancy on the FRN component might very well be driven in part by responses to unexpected reward as well (Holroyd et al., 2008; Walsh and Anderson, 2012). Yet, this effect was found when considering the topography only, and a relatively late time interval (i.e., 298-338 ms following FB onset). Although we failed to find evidence of a systematic change in the explained variance of the FRN-compatible topography with FB expectancy, some cautious is needed in the interpretation of this "null" result. For example, it remains to be tested whether using monetary loss or punishment for the no-reward outcome might not yield stronger modulations of the FRN-compatible topography with expectancy, as this manipulation would necessarily increase the salience of the no-reward outcome (Esber and Haselgrove, 2011). Accordingly, whether or not the FRN-compatible topography varies (in explained variance) with expectancy awaits additional empirical work where other contrasts at the outcome level should be used and compared systematically using similar ERP methods (including loss-related ones and hence the activation of a defensive motivational system; Hajcak and Foti, 2008). Notwithstanding this caveat, our new topographical ERP results are important because they clearly suggest that the processing of FB valence

587 during gambling may obey a two-stage process: first FB valence is evaluated (with no-reward
588 interfering with the default reward-related ERP activity apparently), before a strong expectancy effect
589 comes into play during a later stage and dynamically shapes reward processing, selectively.
590 Presumably, this modulation might reflect the assignment of a different motivational value to the
591 reward-related FB depending on its expectancy. This interpretation aligns well with recent
592 neurophysiological evidence that reveals a specific temporal sequence during evaluative FB processing
593 (Fouragnan et al., 2015; Philiastides et al., 2010): the early (around 220ms post FB onset) categorical
594 evaluation of the outcome (i.e. valence) is later followed (around 300ms) by the processing of its actual
595 deviation relative to the expectation (i.e. salience). More generally, such rapid and fine-grained
596 changes in the actual spatio-temporal dynamic of reward processing during PM could hardly be
597 captured by means of a standard ERP data analysis. Hence, we contend that future ERP studies focused
598 on reward processing and PM should better incorporate this important feature of any ERP component
599 (FRN, RewP, P200, P300 or N200), namely the topography, as it carries relevant information about the
600 complex interplay between FB valence and expectancy. This approach might also help to revise or
601 amend some of the current models available in the field that directly use these specific ERP
602 components to generate testable predictions about the neurophysiology of reward processing and PM
603 (Ullsperger et al., 2014b).

604 Despite its apparent strengths and added value, some limitations related to this topographic
605 ERP mapping analysis warrant comment. Because this approach is based on an estimation (and
606 clustering) of the dissimilarity in terms of spatial configuration of the electric field across successive
607 TFs, it is not suited to reveal the contribution of putative independent components/sources that would
608 be active and compete with one another at the exact same time, for which an ICA or PCA (Foti et al.,
609 2015, 2011; Proudfit, 2015) should preferably be used for example (Eichele et al., 2010). Previously
610 published findings (Holroyd et al., 2008; Proudfit, 2015) suggested that the ERP responses to reward
611 and loss mostly differ by means of a positivity that is unique to reward trials, as opposed to a negativity
612 to no-reward ones. By comparison, the outcome of our ERP topographic mapping analysis suggests the

presence of a phasic FRN-map (characterized by a fronto-central negativity) generated in an early time window following no-reward (around 277ms), which seems to overlap and interfere with a longer-lasting reward-related activity (characterized by a positivity showing a centro-parietal scalp distribution). Tentatively, this discrepancy between our current and these previous ERP studies could be related to the abovementioned methodological factors, as well as the actual incentive used to guide performance monitoring (being sometimes either primarily reward-related or instead loss-related). Presumably, for these reasons our topographic ERP mapping analysis failed to reveal a specific (short-lived) topography associated with reward outcome that would mainly be characterised by a central positivity culminating when the N200 (no-reward) reached its maximum amplitude, as previously suggested for the RewP ERP component (Novak and Foti, 2015; Proudfit, 2015). The RewP topographical map revealed in our study showed instead a broader (central and posterior parietal) and longer-lasting positivity that presumably partly overlapped with the P300 component. Therefore, it remains to determine to which extent the RewP map found in our study corresponds to the RewP ERP component exclusively, or also encompasses the P300 component. Last, it would also be beneficial in future studies to assess whether these two different topographies identified here may also be related somehow to different variations in the spectral content of the EEG/ERP, as recently reward processing has been associated with systematic changes in the power of either theta or delta oscillations (Bernat and Nelson, 2008; Cohen et al., 2007; Marco-Pallares et al., 2008). Considering the ERP results obtained with the different scoring methods used in our study (FRN-m, FRN-pp, or N2 peak) and some dissociations found between them, it appears challenging to relate complex cognitive processes, such as expectancy or reward, to single and temporal-specific ERP deflection, such as the P2 or N2. In this context, a better understanding of the actual neurophysiology of these complex cognitive processes could probably be achieved by supplementing classical ERP analyses with time/frequency methods that can inform about the actual spectral content of the P2-N2-P3 complex, its modulation by reward and expectancy (Cavanagh et al., 2012, 2010; Cohen et al., 2007; Cohen and Donner, 2013; Mas-herrero and Marco-pallarés, 2014; Paul and Pourtois, 2017), and the relative role of phase locked

(captured by ERPs) and non-phase locked oscillatory activity in explaining these effects (see also Cohen and Donner, 2013; Hajihosseini and Holroyd, 2013).

To sum up, the present ERP results advance our understanding of reward processing during gambling (in healthy adult participants) and more specifically how reward is actually shaped by expectancy when the topography, as opposed to amplitude measurements performed at a single scalp location, is carefully considered and properly analysed. Our new results lend support to the existence of two – spatially and temporally – dissociable networks during FB processing. One is driven by no-reward and comprises the dACC, meeting many of the electrophysiological criteria used previously to define the FRN component in the extant ERP literature. The other one competes with the first one, and is primarily reward-related (as well as sensitive to expectancy), sharing in turn many similarities with the RewP. Since abnormal reward processing (and anhedonia) is a cardinal diagnostic feature of several affective disorders, such as major depression, addiction, schizophrenia or pathological gambling, the topographic ERP mapping analysis performed in this study, and meant to explore thoroughly the spatio-temporal dynamic of reward processing during PM, could be used more systematically in the future in clinical settings to elucidate which component of reward processing (in relation to expectancy) could be impaired in these patients, and whether depending on the actual affective disorder being diagnosed, some specific (and stable) topographical ERP anomalies could eventually be evidenced.

Author Note

This work is supported by a Concerted Research Action Grant from Ghent University and by a research grant from the Research Foundation Flanders (FWO). GP is the recipient of an (2015) independent investigator grant awarded by the NARSAD foundation. KP is supported by the FWO (PhD student mandate).

Conflict of interest: none declared.

References

Bernat, E., Nelson, L.D., 2008. Separating Cognitive Processes with Principal Components Analysis of EEG Time-Frequency Distributions Separating Cognitive Processes with Principal Components Analysis of. doi:10.1117/12.801362

Brunet, D., Murray, M.M., Michel, C.M., 2011. Spatiotemporal analysis of multichannel EEG: CARTOOL. Comput. Intell. Neurosci. 2011. doi:10.1155/2011/813870

Bush, G., Luu, P., Posner, M.I., 2000. Cognitive and emotional influences in anterior cingulate cortex. Trends Cogn. Sci. 4, 215–222. doi:10.1016/S1364-6613(00)01483-2

Cavanagh, J.F., Figueroa, C.M., Cohen, M.X., Frank, M.J., 2012. Frontal theta reflects uncertainty and unexpectedness during exploration and exploitation. Cereb. Cortex 22, 2575–2586. doi:10.1093/cercor/bhr332

Cavanagh, J.F., Frank, M.J., Klein, T.J., Allen, J.J.B., 2010. Frontal theta links prediction errors to behavioral adaptation in reinforcement learning. Neuroimage 49, 3198–3209. doi:10.1016/j.neuroimage.2009.11.080

Charrad, M., Ghazzali, N., Boiteau, V., Niknafs, A., 2014. NbClust : An *R* Package for Determining the Relevant Number of Clusters in a Data Set. J. Stat. Softw. 61. doi:10.18637/jss.v061.i06

Cohen, M.X., Cavanagh, J.F., Slagter, H.A., 2011. Event-related potential activity in the basal ganglia differentiates rewards from nonrewards: Temporospatial principal components analysis and source localization of the feedback negativity: Commentary. Hum. Brain Mapp. 32, 2270–2271. doi:10.1002/hbm.21358

Cohen, M.X., Donner, T.H., 2013. Midfrontal conflict-related theta-band power reflects neural oscillations that predict behavior. J. Neurophysiol. 110, 2752–2763. doi:10.1152/jn.00479.2013

Cohen, M.X., Elger, C.E., Ranganath, C., 2007. Reward expectation modulates feedback-related negativity and EEG spectra. Neuroimage 35, 968–978. doi:10.1016/j.neuroimage.2006.11.056

Delorme, A., Makeig, S., 2004. EEGLAB: an open source toolbox for analysis of single-trial EEG dynamics including independent component analysis. J. Neurosci. Methods 134, 9–21. doi:10.1016/j.jneumeth.2003.10.009

Donchin, E., Coles, M.G.H., 1988. Is the P300 component a manifestation of context updating? Behav. Brain Sci. 11, 357. doi:10.1017/S0140525X00058027

Eichele, T., Calhoun, V.D., Debener, S., 2010. Mining EEG-fMRI using independent component analysis 73, 53–61. doi:10.1016/j.ijpsycho.2008.12.018.Mining

Esber, G.R., Haselgrove, M., 2011. Reconciling the influence of predictiveness and uncertainty on stimulus salience : a model of attention in associative learning 2553–2561. doi:10.1098/rspb.2011.0836

Faul, F., Erdfelder, E., Lang, A.-G., Buchner, A., 2007. G*Power 3: A flexible statistical power analysis program for the social, behavioral, and biomedical sciences. Behav. Res. Methods 39, 175–191. doi:10.3758/BF03193146

Ferdinand, N.K., Mecklinger, a., Kray, J., Gehring, W.J., 2012. The Processing of Unexpected Positive Response Outcomes in the Mediofrontal Cortex. J. Neurosci. 32, 12087–12092. doi:10.1523/JNEUROSCI.1410-12.2012

Fiorillo, C.D., Tobler, P.N., Schultz, W., 2003. Discrete Coding of Reward Probability and Uncertainty

by Dopamine Neurons. Science (80-.). 299, 1898–1903.

Foti, D., Weinberg, A., Bernat, E.M., Proudfit, G.H., 2015. Anterior cingulate activity to monetary loss and basal ganglia activity to monetary gain uniquely contribute to the feedback negativity. Clin. Neurophysiol. 126, 1338–1347. doi:10.1016/j.clinph.2014.08.025

Foti, D., Weinberg, A., Dien, J., Hajcak, G., 2011. Event-related potential activity in the basal ganglia differentiates rewards from nonrewards: Response to commentary. Hum. Brain Mapp. 32, 2267–2269. doi:10.1002/hbm.21357

Fouragnan, E., Retzler, C., Mullinger, K., Philiastides, M.G., 2015. Two spatiotemporally distinct value systems shape reward-based learning in the human brain. Nat. Commun. 6, 8107. doi:10.1038/ncomms9107

Fuchs, M., Kastner, J., Wagner, M., Hawes, S., Ebersole, J.S., 2002. A standardized boundary element method volume conductor model. Clin. Neurophysiol. 113, 702–712. doi:10.1016/S1388-2457(02)00030-5

Gabriel, M., Burhans, L., Talk, A., Scalf, P., 2002. The Cingulate Cortex, in: Ramachandran, V.S. (Ed.), Encyclopedia of The Human Brain. Elsevier Science, Amsterdam, pp. 775–791.

Gehring, W.J., Willoughby, A.R., 2002. The medial frontal cortex and the rapid processing of monetary gains and losses. Science (80-.). 295, 2279–2282. doi:10.1126/science.1066893

Gheza, D., De Raedt, R., Baeken, C., Pourtois, G., 2017. ERPs and EEG spectra perturbations reveal integration of reward with effort anticipation during performance monitoring. (Manuscript submitted for pubblication)

Hajcak, G., Foti, D., 2008. Errors Are Aversive Defensive Motivation and the Error-Related Negativity 19, 103–108. doi:10.1111/j.1467-9280.2008.02053.x.

Hajcak, G., Holroyd, C.B., Moser, J.S., Simons, R.F., 2005. Brain potentials associated with expected and unexpected good and bad outcomes. Psychophysiology 42, 161–170. doi:10.1111/j.1469-8986.2005.00278.x

Hajcak, G., Moser, J.S., Holroyd, C.B., Simons, R.F., 2007. It's worse than you thought: The feedback negativity and violations of reward prediction in gambling tasks. Psychophysiology 44, 905–912. doi:10.1111/j.1469-8986.2007.00567.x

Hajihosseini, A., Holroyd, C.B., 2013. Frontal midline theta and N200 amplitude reflect complementary information about expectancy and outcome evaluation. Psychophysiology 50, 550–562. doi:10.1111/psyp.12040

Heydari, S., Holroyd, C.B., 2016. Reward positivity: Reward prediction error or salience prediction error? Psychophysiology 53, 1185–1192. doi:10.1111/psyp.12673

Holroyd, C.B., Coles, M.G.H., 2002. The neural basis of human error processing: Reinforcement learning, dopamine, and the error-related negativity. Psychol. Rev. 109, 679–709. doi:10.1037/0033-295X.109.4.679

Holroyd, C.B., Krigolson, O.E., Lee, S., 2011. Reward positivity elicited by predictive cues. Neuroreport 22, 249–252. doi:10.1097/WNR.0b013e328345441d

Holroyd, C.B., Nieuwenhuis, S., Yeung, N., Cohen, J.D., 2003. Errors in reward prediction are reflected in the event-related brain potential. Neuroreport 14, 2481–2484. doi:10.1097/01.wnr.0000099601.41403.a5

Holroyd, C.B., Pakzad-Vaezi, K.L., Krigolson, O.E., 2008. The feedback correct-related positivity:

Sensitivity of the event-related brain potential to unexpected positive feedback. Psychophysiology 45, 688–697. doi:10.1111/j.1469-8986.2008.00668.x

JASP Team, T., 2017. JASP (Version 0.8.2)[Computer software].

Jurcak, V., Tsuzuki, D., Dan, I., 2007. 10/20, 10/10, and 10/5 systems revisited: Their validity as relative head-surface-based positioning systems. NeuroImage 34, 1600–1611. doi:10.1016/j.neuroimage.2006.09.024

Keil, A., Debener, S., Gratton, G., Junghöfer, M., Kappenman, E.S., Luck, S.J., Luu, P., Miller, G.A., Yee, C.M., 2014. Committee report: Publication guidelines and recommendations for studies using electroencephalography and magnetoencephalography. Psychophysiology 51, 1–21. doi:10.1111/psyp.12147

Knutson, B., Fong, G.W., Adams, C.M., Varner, J.L., Hommer, D., 2001. Dissociation of reward anticipation and outcome with event-related fMRI. Neuroreport 12, 3683–7.

Leech, R., Sharp, D.J., 2014. The role of the posterior cingulate cortex in cognition and disease. Brain 137, 12–32. doi:10.1093/brain/awt162

Lehmann, D., Skrandies, W., 1980. Reference-free identification of components of checkerboard-evoked multichannel potential fields. Electroencephalogr. Clin. Neurophysiol. 48, 609–621. doi:10.1016/0013-4694(80)90419-8

Liu, X., Hairston, J., Schrier, M., Fan, J., 2011. Common and distinct networks underlying reward valence and processing stages: A meta-analysis of functional neuroimaging studies. Neurosci. Biobehav. Rev. 35, 1219–1236. doi:10.1016/j.neubiorev.2010.12.012.

Luck, S.J., Gaspelin, N., 2017. How to get statistically significant effects in any ERP experiment (and why you shouldn't). Psychophysiology 54, 146–157. doi:10.1111/psyp.12639

Luu, P., Tucker, D.M., Derryberry, D., Reed, M., Poulsen, C., 2003. ELECTROPHYSIOLOGICAL RESPONSES TO ERRORS AND FEEDBACK IN THE PROCESS OF ACTION REGULATION 14, 47–53.

Marco-Pallares, J., Cucurell, D., Cunillera, T., Garc??a, R., Andr??s-Pueyo, A., M??nte, T.F., Rodr??guez-Fornells, A., 2008. Human oscillatory activity associated to reward processing in a gambling task. Neuropsychologia 46, 241–248. doi:10.1016/j.neuropsychologia.2007.07.016

Martin, L.E., Potts, G.F., Burton, P.C., Montague, P.R., 2009. Electrophysiological and Hemodynamic Responses to Reward Prediction Violation. Neuroreport 20, 1140–1143. doi:10.1097/WNR.0b013e32832f0dca.Electrophysiological

Mas-herrero, E., Marco-pallarés, J., 2014. Frontal Theta Oscillatory Activity Is a Common Mechanism for the Computation of Unexpected Outcomes and Learning Rate. J. Cogntitive Neurosci. 1–12. doi:10.1162/jocn

Mazziotta, J., Toga, A., Evans, A., Fox, P., Lancaster, J., Zilles, K., Woods, R., Paus, T., Simpson, G., Pike, B., Holmes, C., Collins, L., Thompson, P., MacDonald, D., Iacoboni, M., Schormann, T., Amunts, K., Palomero-Gallagher, N., Geyer, S., Parsons, L., Narr, K., Kabani, N., Le Goualher, G., Boomsma, D., Cannon, T., Kawashima, R., Mazoyer, B., 2001. A probabilistic atlas and reference system for the human brain: International Consortium for Brain Mapping (ICBM). Philos. Trans. R. Soc. Lond. B. Biol. Sci. 356, 1293–1322. doi:10.1098/rstb.2001.0915

Mccoy, A.N., Crowley, J.C., Haghighian, G., Dean, H.L., Platt, M.L., Carolina, N., 2003. Saccade Reward Signals in Posterior Cingulate Cortex 40, 1031–1040.

Michel, C.M., Murray, M.M., 2012. Towards the utilization of EEG as a brain imaging tool. Neuroimage 61, 371–385. doi:10.1016/j.neuroimage.2011.12.039

Michel, C.M., Seeck, M., Landis, T., 1999. Spatiotemporal Dynamics of Human Cognition. Physiology 14, 206–214.

Miltner, W.H.R., Braun, C.H., Coles, M.G.H., 1997. Event-Related Brain Potentials Following Incorrect Feedback in a Time-Estimation Task: Evidence for a "Generic" Neural System for Error Detection. J. Cogn. Neurosci. 9, 788–798. doi:10.1162/jocn.1997.9.6.788

Murray, M.M., Brunet, D., Michel, C.M., 2008. Topographic ERP analyses: A step-by-step tutorial review. Brain Topogr. 20, 249–264. doi:10.1007/s10548-008-0054-5

Nichols, T.E., Holmes, A.P., 2001. Nonparametric Permutation Tests for {PET} functional Neuroimaging Experiments: A Primer with examples. Hum. Brain Mapp. 15, 1–25. doi:10.1002/hbm.1058

Nieuwenhuis, S., Slagter, H. a, von Geusau, N.J.A., Heslenfeld, D.J., Holroyd, C.B., 2005. Knowing good from bad: differential activation of human cortical areas by positive and negative outcomes. Eur. J. Neurosci. 21, 3161–8. doi:10.1111/j.1460-9568.2005.04152.x

Novak, K.D., Foti, D., 2015. Teasing apart the anticipatory and consummatory processing of monetary incentives: An event-related potential study of reward dynamics. Psychophysiology 52, 1470–1482. doi:10.1111/psyp.12504

Pascual-Marqui, R., 2002. Standardized low-resolution brain electromagnetic tomography (sLORETA): technical details. Methods Find. Exp. Clin. Pharmacol. 24, 5–12.

Paul, K., Pourtois, G., 2017. Mood congruent tuning of reward expectation in positive mood: evidence from FRN and theta modulations. Soc. Cogn. Affect. Neurosci. 1–10. doi:10.1093/scan/nsx010

Paul, K., Walentowska, W., Bakic, J., Dondaine, T., Pourtois, G., 2017. Modulatory effects of happy mood on performance monitoring: Insights from error-related brain potentials. Cogn. Affect. Behav. Neurosci. 17, 106–123. doi:10.3758/s13415-016-0466-8

Philiastides, M.G., Biele, G., Vavatzanidis, N., Kazzer, P., Heekeren, H.R., 2010. Temporal dynamics of prediction error processing during reward-based decision making. Neuroimage 53, 221–232. doi:10.1016/j.neuroimage.2010.05.052

Polich, J., Crane Ellerson, P., Cohen, J., 1996. P300, stimulus intensity, and modality. Electroencephalogr. Clin. Neurophysiol. - Evoked Potentials 100, 579–584. doi:10.1016/S0168-5597(96)96013-X

Pourtois, G., Delplanque, S., Michel, C., Vuilleumier, P., 2008. Beyond conventional event-related brain potential (ERP): Exploring the time-course of visual emotion processing using topographic and principal component analyses. Brain Topogr. 20, 265–277. doi:10.1007/s10548-008-0053-6

Proudfit, G.H., 2015. The reward positivity: From basic research on reward to a biomarker for depression. Psychophysiology 52, 449–459. doi:10.1111/psyp.12370

Rouder, J.N., Morey, R.D., Verhagen, J., Swagman, A.R., Wagenmakers, E.-J., 2017. Bayesian analysis of factorial designs. Psychol. Methods 22, 304–321. doi:10.1037/met0000057

Sallet, J., Camille, N., Procyk, E., 2013. Modulation of feedback-related negativity during trial-and-error exploration and encoding of behavioral shifts. Front. Neurosci. 7, 1–10. doi:10.3389/fnins.2013.00209

Sambrook, T.D., Goslin, J., 2015. A neural reward prediction error revealed by a meta-analysis of ERPs using great grand averages. Psychol. Bull. 141, 213–235. doi:10.1037/bul0000006

San Martín, R., 2012. Event-related potential studies of outcome processing and feedback-guided learning. Front. Hum. Neurosci. 6, 1–17. doi:10.3389/fnhum.2012.00304

Schultz, W., 2013. Updating dopamine reward signals. Curr. Opin. Neurobiol. 23, 229–238. doi:10.1016/j.conb.2012.11.012

Schultz, W., Dayan, P., Montague, P.R., 1997. A Neural Substrate of Prediction and Reward. Science (80-.). 275, 1593–1599. doi:10.1126/science.275.5306.1593

Shackman, A.J., Salomons, T. V, Slagter, H.A., Andrew, S., Winter, J.J., Davidson, R.J., 2011. The Integration of Negative Affect, Pain, and Cognitive Control in the Cingulate Cortex. Nat. Rev. Neurosci. 12, 154–167. doi:10.1038/nrn2994.The

Shahnazian, D., Holroyd, C.B., 2017. Distributed representations of action sequences in anterior cingulate cortex : A recurrent neural network approach. doi:10.3758/s13423-017-1280-1

Talmi, D., Atkinson, R., El-Deredy, W., 2013. The Feedback-Related Negativity Signals Salience Prediction Errors, Not Reward Prediction Errors. J. Neurosci. 33, 8264–8269. doi:10.1523/JNEUROSCI.5695-12.2013

Talmi, D., Fuentemilla, L., Litvak, V., Duzel, E., Dolan, R.J., 2012. NeuroImage An MEG signature corresponding to an axiomatic model of reward prediction error. Neuroimage 59, 635–645. doi:10.1016/j.neuroimage.2011.06.051

Tibshirani, R., Walther, G., 2005. Cluster Validation by Prediction Strength. J. Comput. Graph. Stat. 14, 511–528. doi:10.1198/106186005X59243

Towey, J., Rist, F., Hakerem, G., Ruchkin, D.S., Sutton, S., 1980. N250 latency and decision time. Bull. Psychon. Soc. 15, 365–368. doi:10.3758/BF03334559

Ullsperger, M., Danielmeier, C., Jocham, G., 2014a. Neurophysiology of Performance Monitoring and Adaptive Behavior. Physiol. Rev. 94, 35–79. doi:10.1152/physrev.00041.2012

Ullsperger, M., Fischer, A.G., Nigbur, R., Endrass, T., 2014b. Neural mechanisms and temporal dynamics of performance monitoring. Trends Cogn. Sci. 18, 259–267. doi:10.1016/j.tics.2014.02.009

Vaughan, H.G., 1982. The Neural Origins Of Human Event-Related Potentials. Ann. New York Acad. Sci. 125–138.

Vogt, B.A., 2005. Pain and emotion interactions in subregions of the cingulate gyrus. Nat. Rev. Neurosci. 6, 533–44. doi:10.1038/nrn1704

Walsh, M.M., Anderson, J.R., 2012. Learning from experience: Event-related potential correlates of reward processing, neural adaptation, and behavioral choice. Neurosci. Biobehav. Rev. 36, 1870–1884. doi:10.1016/j.neubiorev.2012.05.008

Warren, C.M., Holroyd, C.B., 2012. The impact of deliberative strategy dissociates ERP components related to conflict processing vs. Reinforcement learning. Front. Neurosci. 6. doi:10.3389/fnins.2012.00043

Weinberg, A., Shankman, S.A., 2017. Blunted Reward Processing in Remitted Melancholic Depression. Clin. Psychol. Sci. 5, 14–25. doi:10.1177/2167702616633158

Yeung, N., Botvinick, M.M., Cohen, J.D., 2004. The Neural Basis of Error Detection: Conflict Monitoring and the Error-Related Negativity. Psychol. Rev. 111, 931–959. doi:10.1037/0033-295X.111.4.939

Yu, R., Zhou, W., Zhou, X., 2011. Rapid processing of both reward probability and reward uncertainty

in the human anterior cingulate cortex. PLoS One 6. doi:10.1371/journal.pone.0029633

Figures

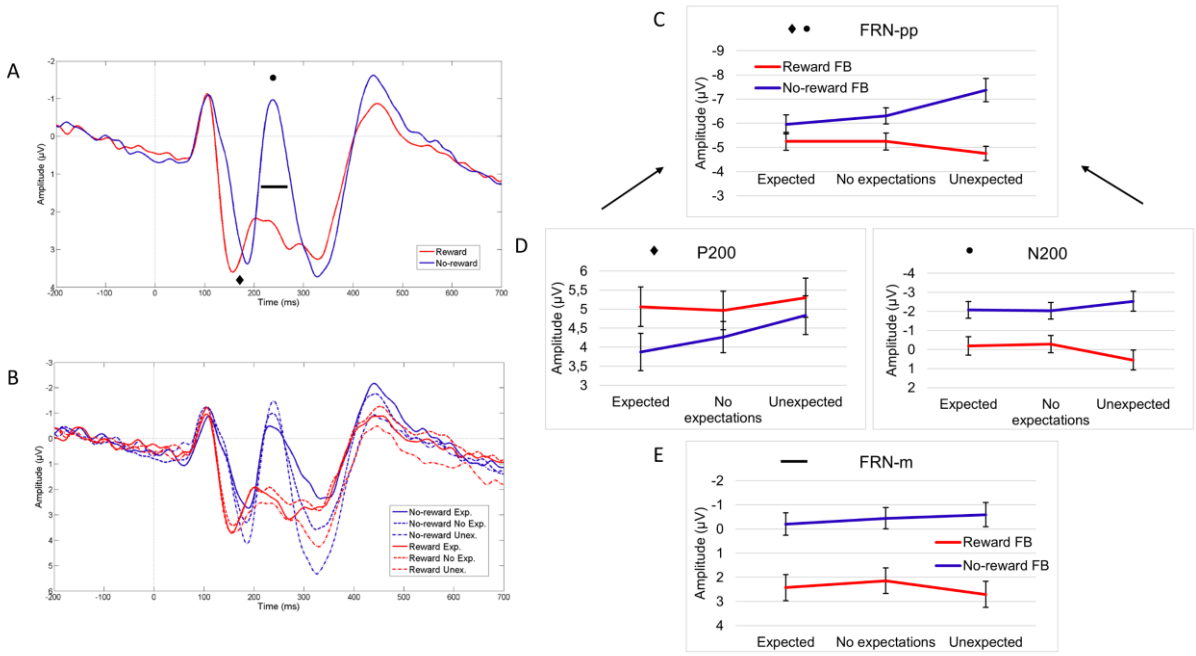

Figure 1. (A) Grand average ERP waveforms computed at FCz for reward and no-reward separately, collapsing across the three levels of FB expectation each time. A conspicuous N200 (giving rise to the FRN component) was elicited for no-reward FB, compared to reward FB. The diamond symbol refers to the preceding P200 (see Figure 1D – left panel for analysis of this component only). The dot symbol refers to the N200 proper (see Figure 1D – right panel for analysis of this component only). The small horizontal black line depicts the fixed interval used when the FRN is measured as mean amplitude (see Figure 1E). The FRN was analyzed using either peak to peak (FRN-pp, using the preceding P200 as initial peak – baseline, see Figure 1C) or as a mean ERP activity (FRN-m, see Figure 1E). (B) Grand average ERP waveforms computed at FCz for all six main conditions. At the N200 level, FB valence interacted with FB expectancy, whereby the N200 was the largest for unexpected negative FB. (C) Mean amplitudes of the FRN when computed peak to peak, showing a significant interaction between FB valence and FB expectancy. (D) Mean amplitudes for P200 (left panel) and N200 (right panel) alone. (E) Mean amplitudes of the FRN when computed using a mean amplitude measurement, showing a main effect of FB valence only. The error bar corresponds to 1 standard error of the mean.

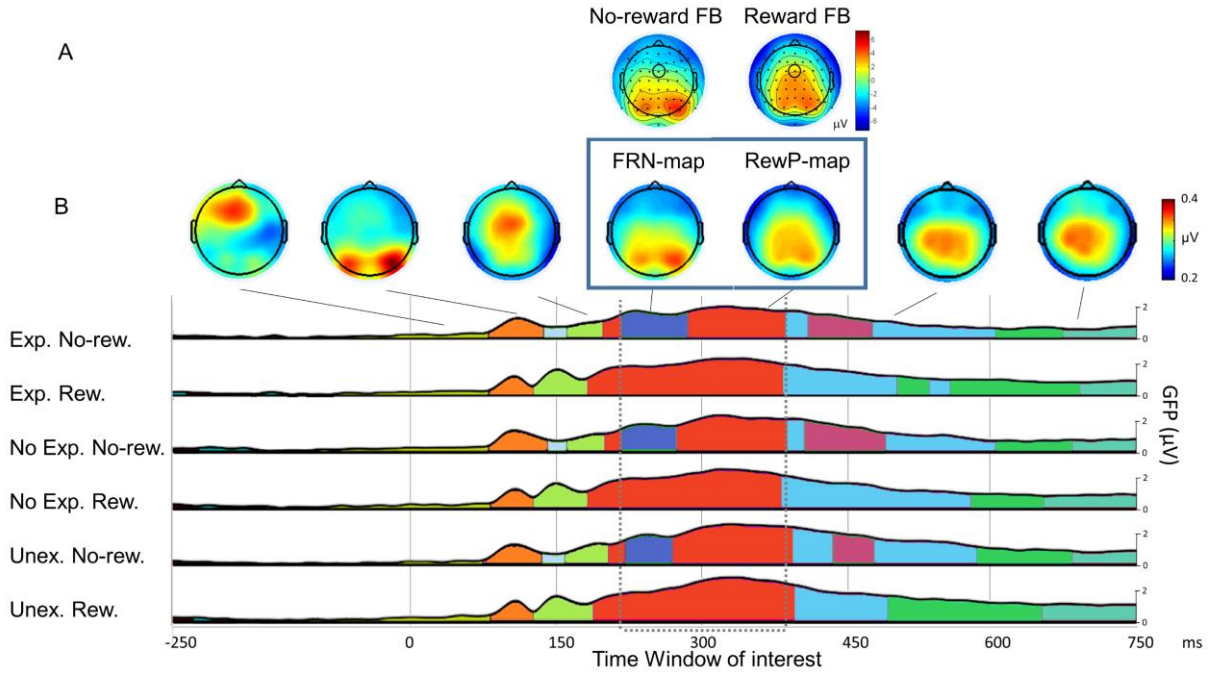

Figure 2. (A) Topographies (voltage maps) of the main ERP activities of interest (irrespective of expectancy), showing the RewP topography (left inset) and the FRN topography (right inset). The circle superimposed of the topographies corresponds to FCz electrode location. Each map is computed as the mean ERP activity during a 50 ms time interval around the N200 peak elicited by no-reward (see Figure 1A). (B) Outcome of the spatio-temporal segmentation of the grand average ERP data (with the six main experimental conditions considered, and showing the entire epoch starting 250 ms prior to and ending 750 ms after feedback onset). A solution with 16 different topographical maps (where only 7 are actually depicted here) was found to explain 93.71 % of the total variance. During the time interval corresponding to the FRN/RewP components, two dissociable activities were evidenced based on FB valence. These two maps had different properties, including a longer duration for the reward-related one, and showed different sensitivity to FB expectancy (see Results section and Figure 3 for results after back fitting to individual subject ERP data).

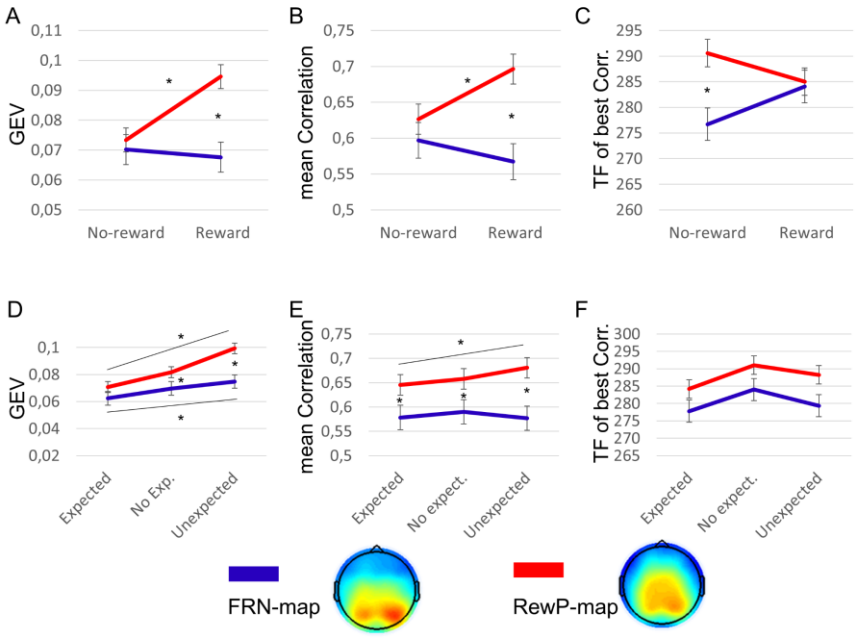

Figure 3. (A-F) Results obtained after fitting back the two dominant maps (FRN and RewP, regardless of expectancy) identified during the clustering step (see Figure 2B) during the 217-386 ms time interval following FB onset to individual subject ERP data, separately for the three main dependent variables used in this analysis: global explained variance (GEV), mean correlation and time-frame (TF) of best correlation. The error bar corresponds to 1 standard error of the mean. For each of them, a significant interaction effect between valence and map was found (A,B), explained by the generation of a reward-specific map for positive feedback, except for the TF of best correlation where a significant earlier time-course was found for the FRN-related map for negative feedback compared to the RewP map (C). (D-E-F) Results obtained after fitting showing differential effect of expectancy on the behavior of the two main maps. While the FRN-related map was weakly modulated by levels of expectancy, such an effect was clearly evidenced for the RewP map that showed a monotonic increase (in GEV or mean correlation) with increasing unexpectedness.

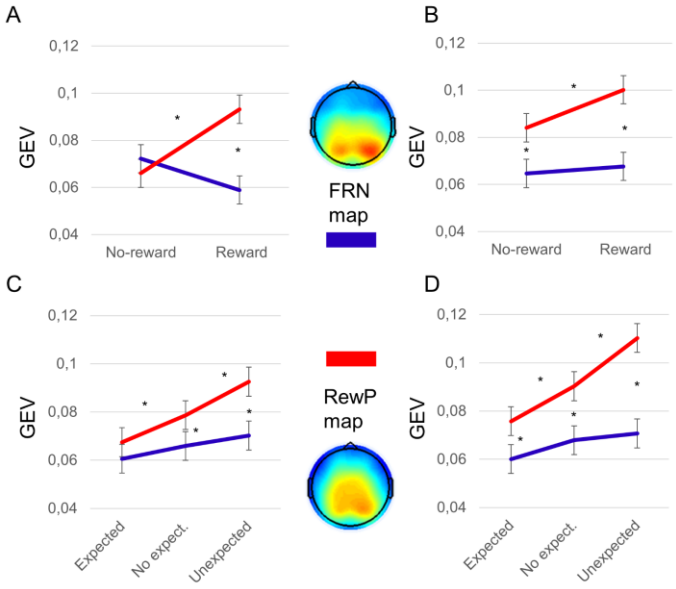

Figure 4. Fitting results (GEV only) shown separately for the early (left column) and late time-window (right column) identified by the main analysis (see Results section for details). Whereas the FRN-map discriminated better no-reward from reward FB during the early time interval (A), the RewP-map discriminated better reward from no-reward FB during the later time interval (B). (C) The FRN-map did not vary with expectancy (in none of the two time intervals). (D) By comparison, the RewP-map varied with expectancy, especially during the later time interval. The error bar corresponds to 1 standard error of the mean.

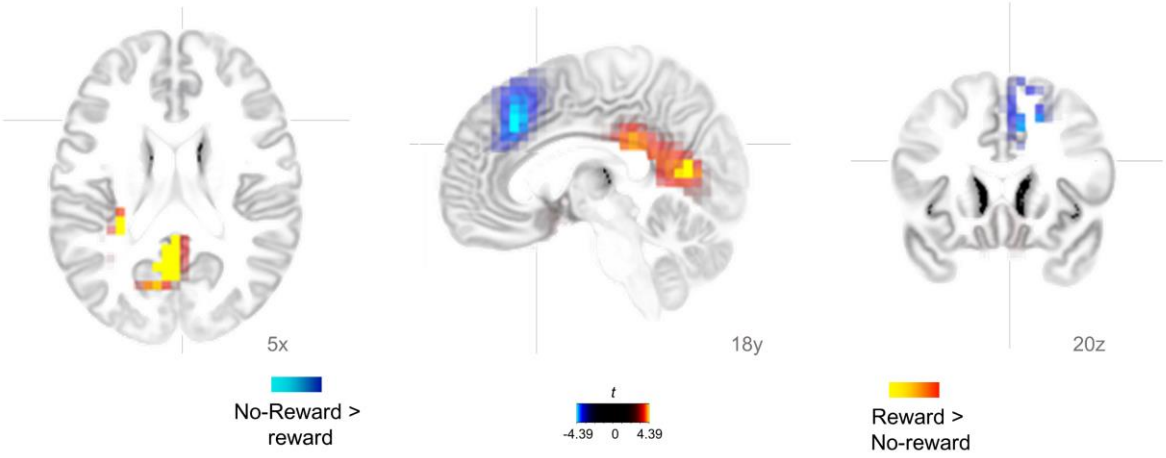

Figure 5. Source localization results. Hot colors provide activations (corrected for multiple comparisons, see Results section for details) for the contrast between reward and no-reward FB, while cold colors provide suprathreshold activations for the reverse contrast. These statistical maps were generated for the mean ERP activity generated within the 217-386 ms time interval following FB onset. No-reward compared to reward yielded activation in the dACC (BA 32; see right inset), spreading to nearby frontal areas (BAs 6, 8, and 9). Conversely, reward compared to no-reward led to activations in the PPC (BA 23; see left inset), spreading to parietal and more ventral regions, including the Precuneus and Parahippocampal gyrus (BAs 23, 27, 29, 30, 13, and 18). It also extended to the left posterior insula (BA 13).